Molecular Biology of the Cell
Vol. 14, 748–763, February 2003

Hepatocyte Growth Factor Switches Orientation of Polarity and Mode of Movement during Morphogenesis of Multicellular Epithelial Structures

Wei Yu,*†§ Lucy E. O'Brien,*†§ Fei Wang,†‡ Henry Bourne,*†‡ Keith E. Mostov,*†§ and Mirjam M.P. Zegers*†‖§

Departments of §Anatomy, *Biochemistry and Biophysics, ‡Cellular and Molecular Pharmacology, and †Cardiovascular Research Institute, University of California, San Francisco, San Francisco, California 94143-0452

Submitted June 19, 2002; Revised October 21, 2002; Accepted October 31, 2002
Monitoring Editor: Peter N. Devreotes

Epithelial cells form monolayers of polarized cells with apical and basolateral surfaces. Madin-Darby canine kidney epithelial cells transiently lose their apico-basolateral polarity and become motile by treatment with hepatocyte growth factor (HGF), which causes the monolayer to remodel into tubules. HGF induces cells to produce basolateral extensions. Cells then migrate out of the monolayer to produce chains of cells, which go on to form tubules. Herein, we have analyzed the molecular mechanisms underlying the production of extensions and chains. We find that cells switch from an apico-basolateral polarization in the extension stage to a migratory cell polarization when in chains. Extension formation requires phosphatidyl-inositol 3-kinase activity, whereas Rho kinase controls their number and length. Microtubule dynamics and cell division are required for the formation of chains, but not for extension formation. Cells in the monolayer divide with their spindle axis parallel to the monolayer. HGF causes the spindle axis to undergo a variable "seesaw" motion, so that a daughter cells can apparently leave the monolayer to initiate a chain. Our results demonstrate the power of direct observation in investigating how individual cell behaviors, such as polarization, movement, and division are coordinated in the very complex process of producing multicellular structures.

INTRODUCTION

One of the most common types of cell polarity is found in polarized epithelial cells, which have an apical surface facing the lumen and a basolateral surface facing other cells and extracellular matrix (Drubin and Nelson, 1996; Mostov *et al.*, 2000). Another category of cell polarity is found in migrating cells, which includes cell movements during development, chemotaxis, wound healing, and metastasis (Nabi, 1999; Franz *et al.*, 2002; Webb *et al.*, 2002). In these types of movement, the cells become polarized in the direction of movement. Migratory polarization seems very different from the seemingly more static polarization of epithelial cells. Nevertheless, epithelial cells can be induced to become motile and assume a morphology and polarization that resembles that of a migratory cell, such as a fibroblast. This occurs during epithelial-mesenchymal transitions that happen in development or oncogenesis (Arias, 2001; Savagner, 2001). Herein, we focus on how cells transition from epithelial polarity to migratory polarity.

One model to address this is to treat polarized epithelial cells, such as Madin-Darby canine kidney (MDCK) cells, with hepatocyte growth factor (HGF) (Birchmeier and Gherardi, 1998). HGF is also known as scatter factor, because it induces MDCK cells grown subconfluently on a solid support to "scatter," i.e., become highly motile (Comoglio and Boccaccio, 2001). The transition from epithelial polarity to migratory polarity can also be studied in cells grown in three-dimensional gels of extracellular matrix, such as type I collagen. These culture conditions may more closely resemble the in vivo environment and have provided useful model systems for studying the formation of multicellular epithelial structures (Cukierman *et al.*, 2001; O'Brien *et al.*, 2002; Zegers *et al.*, 2003).

Article published online ahead of print. Mol. Biol. Cell 10.1091/mbc.E02–06–0350. Article and publication date are at www.molbiolcell.org/cgi/doi/10.1091/mbc.E02–06–0350.

‖ Corresponding author. E-mail address: zegers@itsa.ucsf.edu.

Abbreviations used: CM, conditioned medium; GFP-PH-Akt, fusion of green fluorescent protein with pleckstrin homology domain of Akt; HGF, hepatocyte growth factor; MDCK, Madin-Darby canine kidney; MLC, myosin light chain; MT, microtubule; PI3K, phosphatidyl inositol 3-kinase; P-MLC, phosphorylated myosin light chain; ROCK, Rho kinase

When a single cell suspension of MDCK cells is embedded in such a gel, the cells divide and form spherical cysts, where a monolayer of cells surrounds a central lumen. Cells are polarized, with the apical surface facing the lumen (O'Brien *et al.*, 2001). Treatment of these cysts with HGF causes them to elaborate branching tubules. This process involves a complex series of changes in cell polarity and movement (Montesano *et al.*, 1991a,b; Metzger and Krasnow, 1999; Hogan and Kolodziej, 2002; O'Brien *et al.*, 2002). HGF-induced tubulogenesis can be divided into four stages, termed extensions, chains, cords, and tubules (Pollack *et al.*, 1997, 1998). Approximately 6–12 h after addition of HGF some cells produce extensions, large pseudopods protruding from their basolateral surface. These cells retain a small apical surface and are thus part of the monolayer. At ~24 h, chains of one to three cells protrude from the cyst. At this stage, cells have lost apico-basal polarity. Subsequently, chains transform into cords two to three cells thick. Small lumens lined by newly established apical surfaces form between cells. These lumens expand to ultimately form a single lumen contiguous with the lumen of the original cyst, marking the completion of mature tubules.

Herein, we have studied the early stages in which the cells in the monolayer of the cyst wall form extensions and chains, because these may correspond to the transition from epithelial polarity to the polarity of a migrating cell. These stages also involve cell movement, because formation of extensions involves movement of a portion of the cell, and formation of chains involves movement of entire cells away from the cyst. To analyze the mechanisms underlying extension and chain formation, we examined four classes of molecules and processes that are known to be involved in polarization and movement in other systems. 1) Phosphatidyl inositol 3 kinase (PI3K). We found that the products of PI3K are concentrated at the leading edge in extensions and that PI3K is needed for extension formation. 2). Microtubules. Surprisingly, microtubule dynamics is not needed for extension formation. 3). The Rho effector, Rho kinase (ROCK). We found that ROCK determines the number and length of extensions. 4). Cell division. Cell division is not needed for extension formation but is required for making chains. As cells divide and migrate out to form chains, they change the orientation of their division from parallel to the plane of the monolayer to roughly perpendicular to this plane. This is an example of an oriented cell division in an experimentally tractable mammalian system, which should facilitate future analysis of this important process.

MATERIALS AND METHODS

Cell Culture, Cystogenesis, and Tubulogenesis

MDCK cells were maintained in minimal essential medium containing Earle's balanced salt solution (Cellgro; Mediatech, Herndon, VA) supplemented with 5% fetal bovine serum (Hyclone Laboratories, Logan, UT), 100 unit/ml penicillin, 100 μg/ml streptomycin (control medium below) in 5%CO_2, 95% air. For growth of cells in three-dimensional collagen gels, cells were trypsinized and then triturated at room temperature into a single-cell suspension of 4×10^4 cells/ml in type I collagen solution containing 66% vitrogen 100 (3 mg/ml; Cohesion Technologies, Palo Alto, CA) (Pollack *et al.*, 1998; O'Brien *et al.*, 2001). Cells in suspension were plated onto Nunc Anopore filters (10 mm in diameter, 0.02-μm pore size). The collagen mixture was incubated for 30 min at 37°C, 5%CO_2, 95% air to allow the collagen to gel and then control medium was added. Cells were fed every 3 d and grown for 7–10 d until cysts with lumen were formed. For tubulogenesis, 7-d-old cysts were stimulated with 1:1 conditioned medium (CM) containing HGF from MRC5 human lung fibroblasts: control medium.

Cell Transfection

Early passage MDCK cells grown to ~30% confluence on 10-cm plastic dishes were transfected with 20 μg of a cDNA expression vector encoding green fluorescent protein (GFP)-α-tubulin (BD Biosciences Clontech, Palo Alto, CA), GFP-pleckstrin homology (PH)-Akt (Servant *et al.*, 2000), or GFP-myosin light chain (MLC), according to previously published protocols (Breitfeld *et al.*, 1989; Lipschutz *et al.*, 2001). Transfected cells were replated in medium containing 700 μg/ml G418 72 h after transfection. Medium was changed every 3–4 d. After 12 d of G418 selection, surviving cloned were picked and screened for GFP expression. Clones expressing GFP-tagged proteins were detected by observation with a confocal laser scanning microscope and Western blot with anti-GFP antibody diluted at 1:1000. One clone of each that formed cysts in collagen gel was chosen for use. All cell lines were kept under selection with G418.

Antibodies and Reagents

The primary antibodies used in this study were mouse anti-cis-Golgi enzyme GM130 (Transduction Laboratories, Lexington, KY), mouse anti-α-tubulin antibody (Sigma-Aldrich, St. Louis, MO), and goat anti-P-MLC (Thr18,Ser19) and rabbit-anti-MLC (Santa Cruz Biotechnology, Santa Cruz, CA). Secondary antibodies used were anti-mouse Alexa 594 (Molecular Probes, Eugene, OR). Actin filaments were stained with Alexa Fluor 488 phalloidin (Molecular Probes). Nuclei were labeled with TOPRO-3 (Molecular Probes). Reagents used in this study were nocodazole and LY29004 (Sigma-Aldrich), mitomycin C and Y27632 (Calbiochem, San Diego, CA), and G418 (Invitrogen, Carlsbad, CA).

Western Blot Analysis of MLC Levels

MDCK cells were grown to confluence in 24-mm-diameter wells and then treated with CM, CM with 30 μM Y27632, and Y27632 for 16 h, respectively. Cells were lysed in 500 μl of Triton X-100 lysis buffer (10 mM triethanolamine, pH 7.4, 1.0% Triton X-100, 0.1% SDS, 100 mM NaCl, 1 mM EDTA, 1 mM EGTA, 1 mM NaF, 20 mM Na_4P2O_7 and 2 mM Na_3VO_4). Lysates were boiled for 5 min and cleared by centrifugation. Protein concentrations were determined by a bicinchoninic acid protein assay (Pierce Chemical, Rockford, L), and equal amounts of proteins were electrophoresed on 4–15% SDS-PAGE gels (Bio-Rad, Hercules, CA), immunoblotted, and detected with an enhanced chemiluminescence system (PerkinElmer Life Sciences, Boston, MA)

Treatment of MDCK Cysts with Reagents

LY294002. Seven-day-old MDCK cysts were incubated with 20 μM LY294002 in CM at 37°C for 16 h. As a control, cysts were treated with CM only for 16 h. For chain formation, cysts were treated with CM for 16 h to produce extensions and then treated with 20 μM LY294002 in CM.

Nocodazole. Seven-day-old cysts were preincubated at 4°C for 1 h and then incubated in 200 ng/ml nocodazole in CM at 37°C for 16 or 40 h separately. As a control, cysts were treated with only CM for 16 or 40 h, without the 4°C incubation. To arrest cells at a mitotic stage during tubule formation, cysts were stimulated with CM for 72 h and then incubated in 200 ng/ml nocodazole for an additional 24 h.

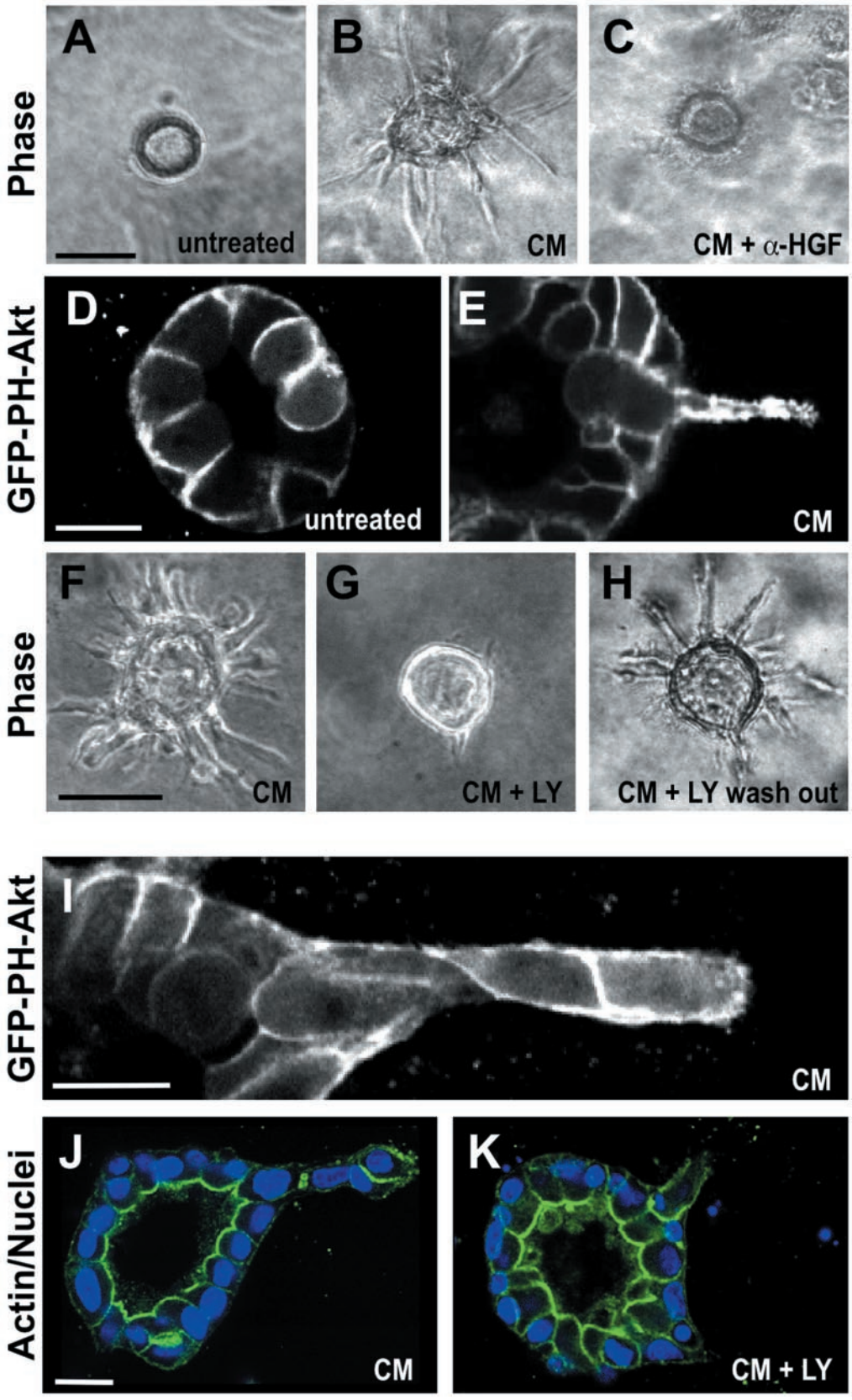
Phase
A
untreated
B
CM
C
CM + α-HGF
GFP-PH-Akt
D
untreated
E
CM
Phase
F
CM
G
CM + LY
H
CM + LY wash out
GFP-PH-Akt
I
CM
Actin/Nuclei
J
CM
K
CM + LY

Mitomycin C. Seven-day-old cysts were preincubated with 0.5 ng/ml mitomycin C at 37°C overnight and then treated with mitomycin C in CM at 37°C for 16 or 40 h, respectively. As control, cysts were treated with CM only for 16 or 40 h.

Immunofluorescence Staining

The procedure for the immunofluorescence staining was described in detail in previous publications (Pollack *et al.*, 1998; O'Brien *et al.*, 2001). All samples were rinsed with phosphate-buffered saline+ twice quickly and then treated with collagenase type VII (Sigma-Aldrich) at 37°C for 10 min. Cysts were fixed with 3% paraformaldehyde for 30 min and with 0.25% Triton X-100 for 10 min at room temperature, and then quenched with 50 mM NH_4Cl for 10 min and permeabilized with 0.1% saponin and 0.7% gelatin for 30 min. Samples then were incubated in primary antibodies at 4°C for overnight. After sufficient washing, samples were treated with 0.1 mg/ml RNase at 37°C for 10 min and then incubated in Alexa 594-conjugated secondary antibody 1:200 dilution and Alexa Fluo 488-phalloidin at 1:50 dilution at 4°C overnight. After washing, cysts were stained for nuclei with TOPRO3 at 1:500 dilution at 37°C for 1 h. All samples were mounted with Prolong medium (Molecular Probes) and then dried at room temperature overnight.

Time-Lapse Images

Cells expressing GFP-α-tubulin were grown in three-dimensional collagen gels as described above. Coverglass-bottomed chambers (Nalge Nunc, Naperville, IL) coated with Sigmacote (Sigma-Aldrich) were used for growing cysts to obtain live cell images. After 7 d of culture, cysts were incubated in phenol red-free medium for 48 h and then fed with phenol red-free Leibovitz's L-15 medium to permit incubation in room air (Invitrogen) with 1% antibiotic and 5% fetal bovine serum for 2 d. Therefore, we used recombinant human HGF (rhHGF; generous gift of R. Schwall, Genentech, South San Francisco, CA) in these experiments, because the buffer components in CM were not compatible with live cell imaging. Cysts treated with rhHGF (100 ng/ml) 8 h or with no treatment were observed with a 510 confocal microscope (Carl Zeiss, Jena, Germany) by using an Argon laser and 60× water immersion lens. Temperature was maintained at 37°C by using a temperature-controlled stage. Once dividing cells were found, time-lapse images were collected as TIFF files and then analyzed with NIH 1.62 and Adobe PhotoShop software.

Image Analysis

Phase-contrast pictures were taken by a digital camera (Hamamatsu, Bridgewater, NJ) equipped with an Aviovert 100 microscope (Carl Zeiss) by using Open Lab software. Images were then converted to PhotoShop format. Quantitation of the number of extensions was as described previously (Pollack *et al.*, 1997; Lipschutz *et al.*, 2000). Immunofluorescence stained samples were observed with a 1024 confocal laser scan microscope (Bio-Rad) equipped with an Eclipse TE microscope (Nikon, Tokyo, Japan) or on two different 510 LSM confocal microscopes (Carl Zeiss), one of which was equipped with a heated stage. Images were collected as Raw files and then analyzed with PhotoShop software.

RESULTS

Role of PI3K in Extensions and Chains

PI3K is implicated in the polarization of chemotaxing neutrophils, *Dictyostelium*, and fibroblasts (Firtel and Chung, 2000; Haugh *et al.*, 2000; Servant *et al.*, 2000; Comer and Parent, 2002; Wang *et al.*, 2002). In these cells the phospholipid products of PI3Ks asymmetrically accumulate at the plasma membrane of the leading edge. In contrast, during astrocyte wound healing, polarization and migration of the cells at the wound edge is independent of PI3K (Etienne-Manneville and Hall, 2001).

PI3K is known to be activated by HGF (Khwaja *et al.*, 1998; Kamikura *et al.*, 2000). To investigate how PI3K may act in a localized manner during specific stages of HGF-induced tubulogenesis, we made an MDCK cell line expressing GFP fused to the pleckstrin homology domain of Akt (GFP-PH-Akt), which was used as a probe for phospholipid products of PI3K (phosphatidyl inositol-3,4-P_2 and -3,4,5-P_3). To simulate cells with HGF, we usually used medium that had been conditioned by MRC5 fibroblasts (conditioned medium, CM). CM contains high concentrations of HGF, which is the tubulogenesis-promoting activity in CM (Figure 1, A and B) (Montesano *et al.*, 1991a,b). Indeed, when we added 2.5 μg/ml neutralizing anti-HGF antibodies to the CM, tubulogenesis was completely abolished (Figure 1C). We found that in control cysts GFP-PH-Akt was uniformly localized at the basolateral membrane but was excluded from the apical surface (Figure 1D). A similar localization of this probe was previously observed in MDCK cells grown as a monolayer on filters (Watton and Downward, 1999), (Montesano *et al.*, 1991a,b). In cells that had been treated with CM for 16 h and formed extensions, GFP-PH-Akt strikingly accumulated in extensions, thus suggesting a possible involvement of PI3K in extension formation (Figure 1E).

Next, we treated cysts with a specific inhibitor of PI3K, LY294002. At 20 μM, LY294002 strongly inhibited the formation of extensions and resulted in cysts that formed only a very few short and thin extensions (compare Figure 1, F and G). Similar results were obtained after treatment with 25 μM wortmannin (our unpublished data). Moreover, extension formation in LY294002 and wortmannin treated cells (our unpublished data) was fully restored upon washout of the drugs (Figure 1H), which argues against the possibility that the effects of the drugs were due to toxicity or induction of apoptosis. These findings suggest a requirement for PI3K during extension formation.

We also examined the localization of GFP-PH-Akt in cells that had been treated with CM for 40 h to allow the formation of chains. In contrast to unstimulated cells in cysts or CM-stimulated cells containing extensions, cells in chains had GFP-PH-Akt uniformly around the entire plasma membrane (Figure 1I). To test the role of PI3K in chain formation,

Figure 1 (facing page). Role of PI3K in HGF-induced extension and chain formation. (A–C) Phase contrast images. (A) Untreated cyst. (B) Cyst treated with CM for 16 h to allow formation of extensions. (C) Cyst treated with CM for 16 h in the presence of 2.5 μm/ml anti-rhHGF IgG, which inhibits formation of extensions. (D and E) Confocal fluorescence images of cysts expressing GFP-PH-Akt. (D) Untreated cyst. (E) Cyst expressing GFP-PH-Akt stimulated with CM for 16 h to allow formation of extensions. (F–H) Phase contrast images. (F) Cyst treated with CM for 16 h. (G) Cyst treated with CM for 16 h in the presence of 20 μM LY294002. (H) Cyst treated with CM and 20 μM LY294002 for 16 h, followed by a washout of LY294002, and subsequent treatment with CM for another 24 h. (I) Fluorescence image of cyst expressing GFP-PH-Akt, stimulated with CM for 40 h to allow formation of chains. (J) Cyst stimulated with CM for 40 h to produce a chain. Fluorescent phalloidin in green, blue is nuclei. (K) Cyst stimulated with CM for 16 h and then treated with CM and 20 μM LY294002 for an additional 24 h. Staining as in J. Bars, 50 μm in A, B, C, F, G, and H and 10 μm in D, E, I, J, and K.

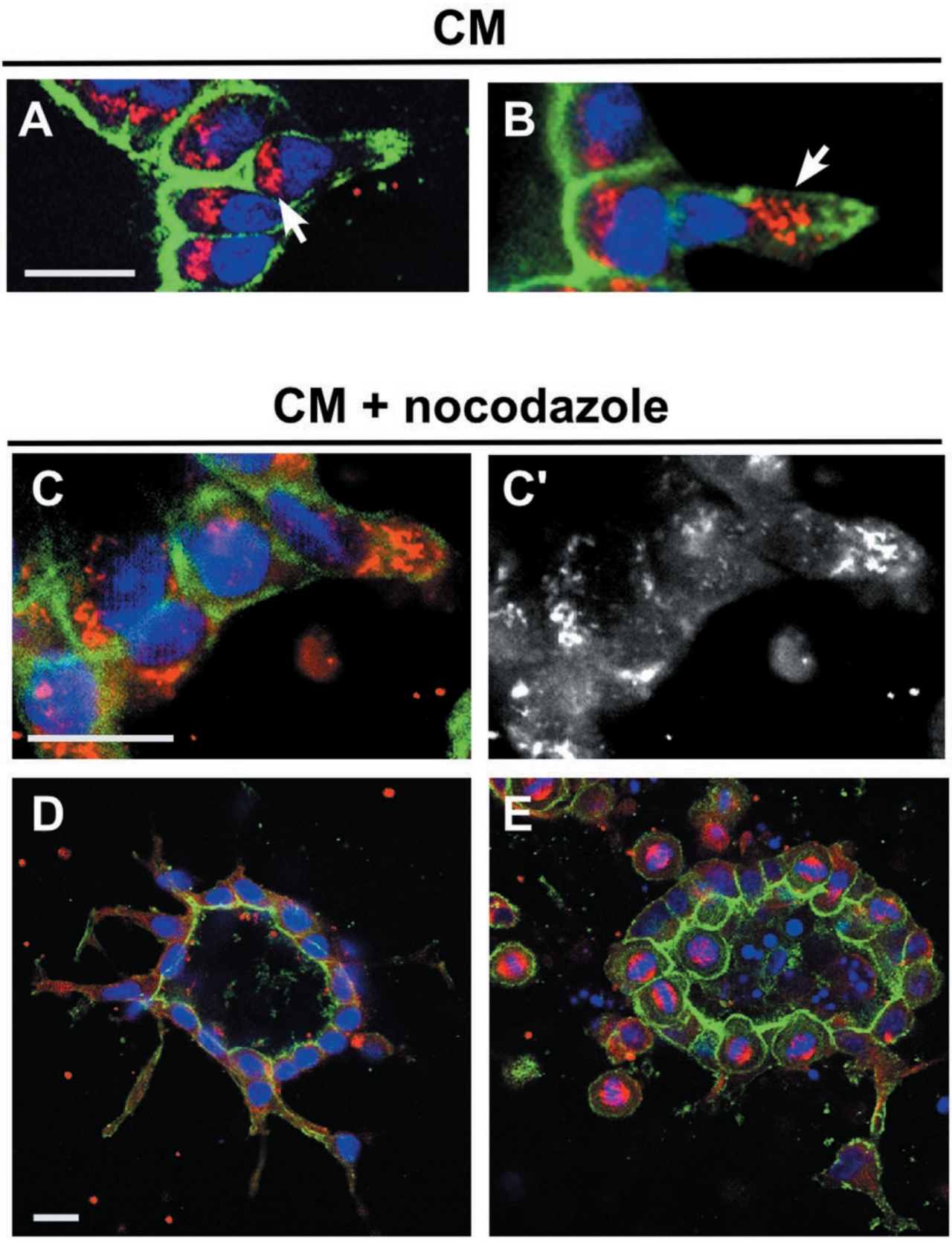
CM
A
B
CM + nocodazole
C
C'
D
E

we first treated cysts with CM for 16 h to produce extensions and then incubated the cysts for an additional 24 h in the continued presence of CM and in the concurrent absence or presence of LY294002. As expected, in the absence of LY294002 the extensions went on to form chains (Figure 1J). However, in the presence of LY294002, no chains and indeed very few extensions were seen (Figure 1K). Presumably, the LY294002 caused the extensions that had formed to collapse.

Golgi Orientation

During migration of several cell types, such as fibroblasts, T cells, and astrocytes, the Golgi apparatus reorients toward the leading edge (Schliwa and Hõner, 1993; Stowers *et al.*, 1995; Nobes and Hall, 1999; Etienne-Manneville and Hall, 2001). This may facilitate the delivery of biosynthetic and perhaps recycling vesicles to the growing region of plasma membrane. It was therefore interesting to ask whether the Golgi similarly reoriented toward the leading edge of extensions and/or chains. As described previously, in control cysts the Golgi is located beneath the apical surface, i.e., between the nucleus and the apical surface (Figure 2A) (O'Brien *et al.*, 2001). Surprisingly, for treatment with CM for 16 h in cells that remained in the cyst wall and had extensions, the Golgi did not reorient toward the leading edge of the extension. Rather, in 100% (n = 30) of such cells, the Golgi remained under the apical surface (Figure 2B). Some of these cells had only very small apical surfaces remaining and the nuclei were starting to move away from the cyst. In contrast, after 40 h of CM, for cells in chains (i.e., no detectable apical surface), the Golgi frequently reoriented. For cells at the tip of the chain, in 69% the Golgi was now orientated at the leading edge (example shown in Figure 2B), whereas in only 18% the Golgi was still facing toward cyst wall, and in 13% the Golgi was at the sides of the cell (n = 61). In cells located at the middle of the chains (i.e., neither in cyst wall nor at the tip of the chain), the Golgi was apparently randomly located (31% toward the tip, 36% at the sides, 33% located toward the cyst wall, n = 45).

Figure 2 (facing page). Orientation of the Golgi in extensions and chains and effect of nocodazole on extension and chain formation. (A) Cyst treated with CM for 16 h to produce extension. Golgi marker (GM130) is red, fluorescent phalloidin is green, and nuclei are blue. One cell has formed an extension and has a concentration of actin at the tip of this extension, near the right edge of the panel. This cell still has a small apical surface, which is at the base of a deep indentation of the cyst lumen. Note that the Golgi in this cell is still underneath the apical surface (arrow). (B) Cyst treated with CM for 40 h to form a short chain. The cell in the chain has left the monolayer. Note that the nucleus is close to the nucleus of a cell that remains in the monolayer. Arrow indicates the Golgi in this chain cell, which is oriented toward the leading edge of the cell, away from the cyst. (C and C′) Disassembly of the Golgi in nocodazole-treated extension. Cyst was preincubated for 1 h at 4°C and then treated for 16 h with CM and 200 ng/ml nocodazole. (C) Staining as in A. C′ emphasizes fragmented Golgi by GM130 staining alone. (D) Cyst was preincubated for 1 h at 4°C and then treated for 16 h with CM and 200 ng/ml nocodazole. Green is fluorescent phalloidin, blue is nuclei, and red is microtubules. Fairly normal extensions are seen. (E) As in D, except treatment was for 40 h. Note many cells arrested in mitosis (red spindles) in and around the cyst. Bar, 10 μm.

Role of Microtubule Dynamics

The Golgi is often located near the centrosome or microtubule organizing center, and its localization can be used as a marker for the location of the microtubule organizing center. The centrosome reorients during migration of some types of cells (e.g., Chinese hamster ovary) but not others (e.g., PtK) (Yvon *et al.*, 2002). Given the changes in localization of the Golgi, we asked whether dynamic changes in microtubules (MTs) play a role in formation of extensions and chains (Wittmann and Waterman-Storer, 2001). Although the MTs in polarized epithelial cells are relatively stable and resistant to depolymerization by nocodazole, low concentrations of this drug (e.g., 200 ng/ml) can block MT dynamics (Vasquez *et al.*, 1997). Cysts were preincubated at 4°C for 1 h and then incubated at 37°C with CM for 16 or 40 h, in the presence or absence of 200 ng/ml nocodazole. The number of cells with mitotic figures, most with normal-looking spindles, increased 13- and 41-fold after a 16- and 40-h nocodazole treatment, respectively, thus confirming that the nocodazole was inhibiting MT dynamics. (Higher concentrations of nocodazole produced abnormal spindles.) Inhibition of MT dynamics was furthermore apparent from a fragmented Golgi (Figure 2, C and C′). At 16 h, cysts treated with nocodazole had formed extensions, which were similar in number, size, and shape to those in the minus nocodazole control (Figure 2, C and D, compare with control in Figure 1, B and E). However, at 40 h no chain formation was observed. Some isolated, rounded cells are seen outside of the cyst, but these do not seem to be in contact with each other or with the cyst (Figure 2E). These cells seem to arrested in mitosis, due to the inhibition of MT dynamics by nocodazole. This is in contrast to the well-formed chains seen in controls treated with CM alone for 40 h (Figure 1, I and J).

Role of the Actin Cytoskeleton and Rho Kinase

We observed that the formation of both extensions and chains was blocked by the actin inhibitors latrunculin B and jasplakinolide (our unpublished data). The function of the actin cytoskeleton in cell polarity and movement is regulated by small GTPases of the Rho family, such as Rho, Rac, and Cdc42 (Bishop and Hall, 2000; Ridley, 2001).

We have previously reported that a dominant negative form of Rac1 causes an inversion of the polarity of cysts (O'Brien *et al.*, 2001) and prevents tubulation in response to HGF (O'Brien and Mostov, unpublished data). We have found similar results with a dominant negative version of Cdc42 (Datta and Mostov, unpublished data). To investigate the role of RhoA in extension and chain formation, we used the drug Y27632, which blocks a major class of RhoA effectors, ROCK I and ROCK II (Uehata *et al.*, 1997). ROCK is necessary for maintaining a cortical actin-myosin network and for formation and contractility of stress fibers (Nobes and Hall, 1999). We first treated cells with 30 μM Y27632 alone for 24 h. Although the treated cysts looked nearly normal by phase contrast microscopy (our unpublished data), confocal microscopy by using fluorescent phalloidin showed the presence of very short basolateral extensions (compare Figure 3A, control, with E, Y27632 treated). These extensions were visible as early as 3 h after treatment with Y27632 and were comparable to the extensions seen with a 3-h treatment of CM alone (our unpublished data). How-

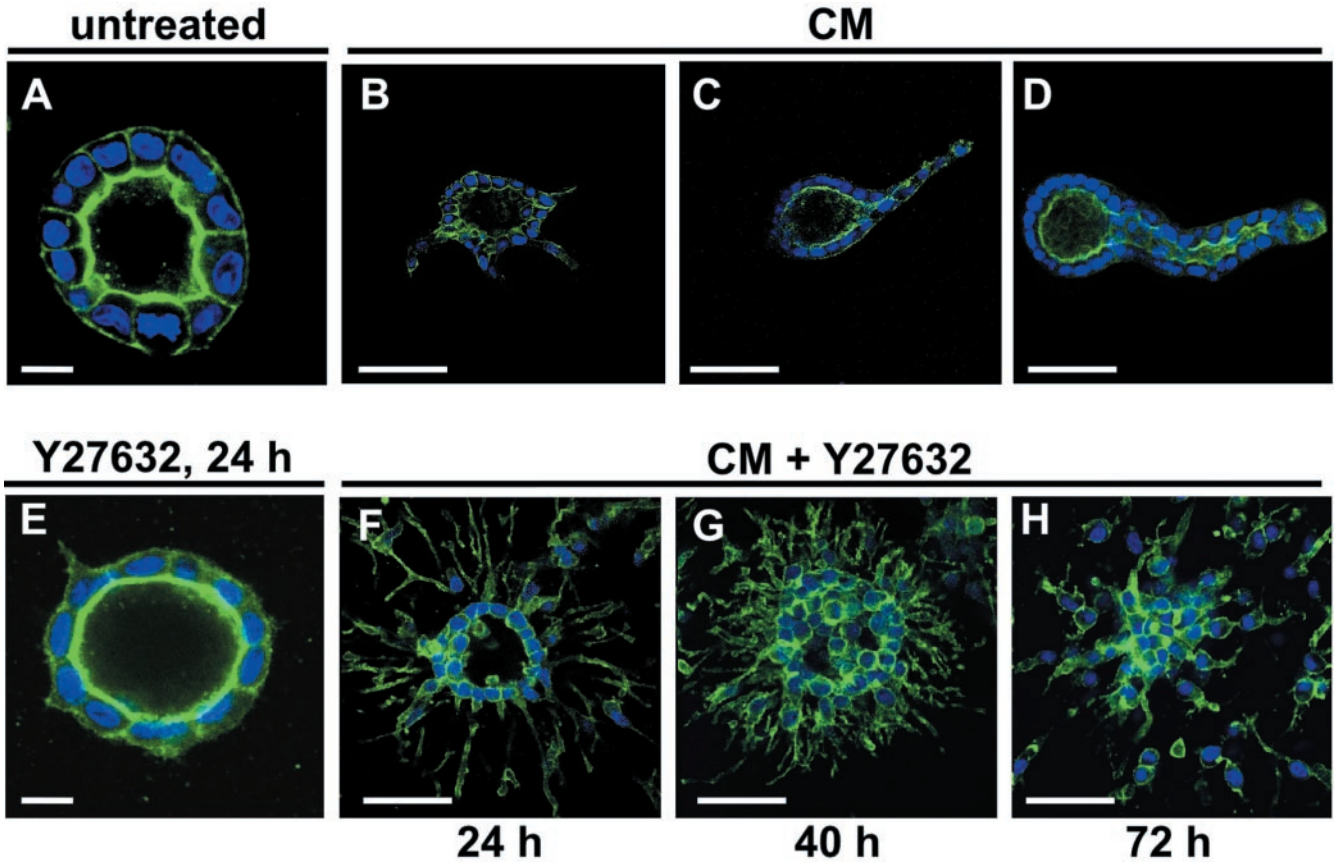

Figure 3. Involvement of ROCK in extension and chain formation. Confocal micrographs of cysts. Phalloidin staining in green, nuclei in blue. (A) Untreated cyst. (B, C, and D) Cysts treated with CM for 24, 40, or 72 h, respectively. (E) Cyst treated with 30 μM Y27632 for 24 h. (F–H) Cysts treated with CM and Y27632 for 24, 40, or 72 h, respectively. Bars, 10 μm in A and E; 50 μm in all other panels.

ever, the CM-only extensions continued to grow, whereas the Y27632-only extensions apparently remained the same length at times >3 h (our unpublished data).

When cells were treated with CM and 30 μM Y27632 for 24 h, we noticed a dramatic increase in the number and the length of extensions (Fig, 3, compare B with F) The number of extensions at 24 h increased ~9.5-fold (n = 59 cysts for CM alone, n = 35 for CM + Y27632). The mean extension length with CM alone was 32.2 ± 5.0 (SD) μm, and 67.8 ± 8.4 μm with Y27632 + CM (n = 55 extensions in each group). Taken together, these data suggest that ROCK normally restricts the number and length of extensions. We also examined the effect of Y27632 on chain formation. In cysts treated for 40 or 72 h with CM and Y27632, cells migrated out of the cysts (Figure 3, compare C with G and D with H). However, the cells lost contact with their neighbors and formed isolated cells (Fig. 3, G and H). Chains were not seen.

Strikingly, in addition to migrating away from the cyst, some cells migrated into the center of the cyst after 24 h (Figure 3F), and by 40–72 h the lumen of the cyst was obliterated by cells that had migrated into it (Figure 3, G and H). This suggests that Y27632 disrupts the directional mechanism that normally causes the cells to migrate only away from the cyst and instead allows them to migrate in multiple directions.

ROCK has several known substrates. One of its major substrates is myosin phosphatase, which results in elevated phosphorylated myosin light chain (P-MLC) (Kimura *et al.*, 1996). P-MLC is in turn correlated with assembly of myosin II filaments and activation of myosin ATPase activity (Chrzanowska-Wodnicka and Burridge, 1996). MLC may also be a substrate of ROCK (Amano *et al.*, 1996). We used a goat antibody that is specific for P-MLC (phosphorylated on Thr18 and Ser19) to localize the P-MLC. In cells in the monolayer of the cyst wall, of untreated cyst most of the P-MLC signal is at the basal surface (Figure 4A), coincident with the actin stress fibers that underlie the basal surface (our unpublished data). Some of the P-MLC is concentrated apically, in the area of tight junctions (arrowheads).

We were unable to localize total endogenous MLC, because the available antibodies did not work for immunocytochemistry on cysts embedded in thick collagen gels. We therefore expressed a GFP-MLC fusion, which has been shown to localize similarly to endogenous MLC (Ward *et al.*, 2002). This GFP-MLC localized mainly to the basal surface, although a small amount localized to the apical region, similar to P-MLC (Figure 4, A′ and A″, arrowheads). We were able to measure the total amount of MLC by using a Western blot, and this did not change with CM and/or Y27362 (Figure 4H).

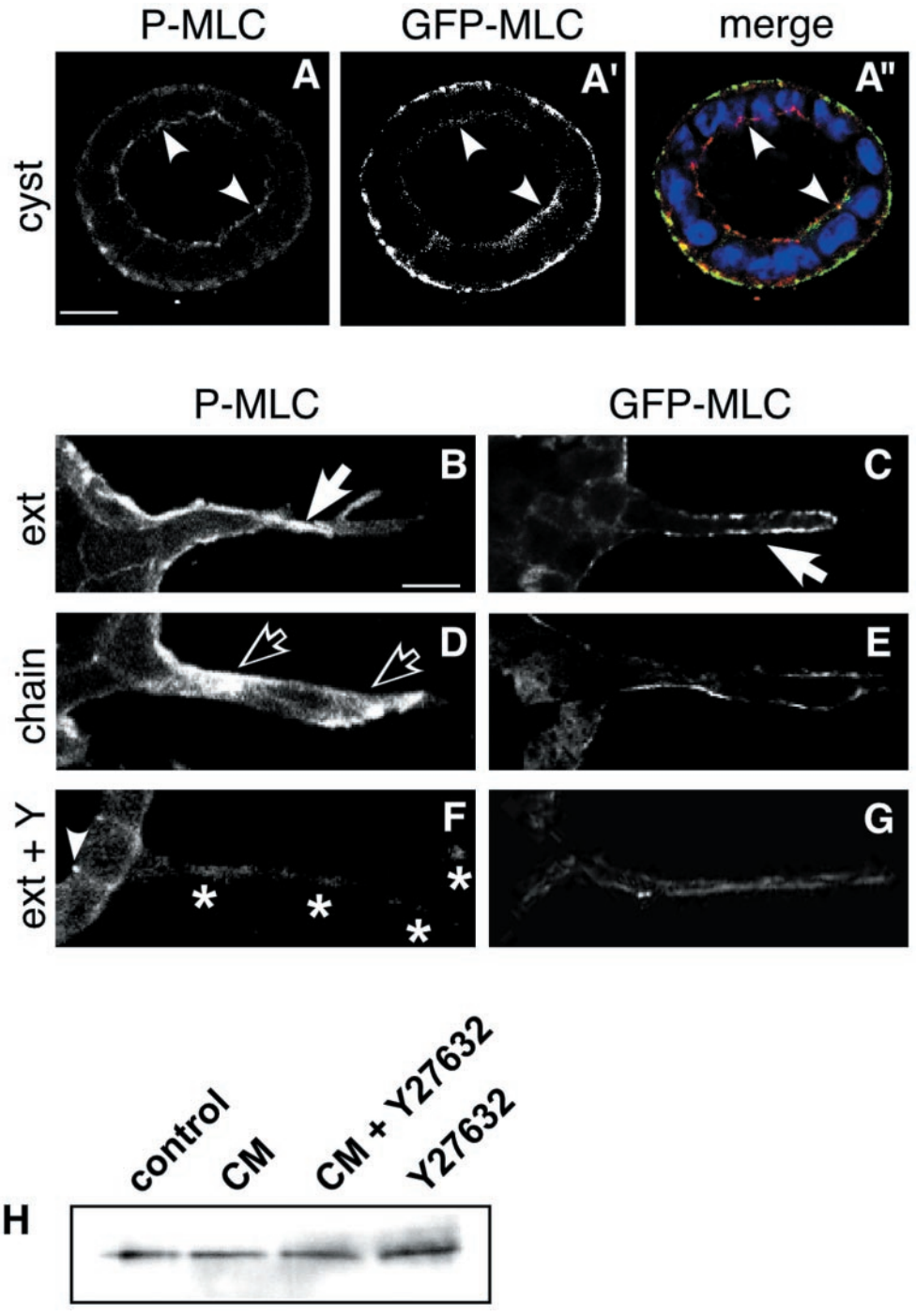

Figure 4. Localization of P-MLC and GFP-MLC. (A, A′, and A″) Confocal micrograph of untreated cyst. P-MLC (A, red in merge A″). Arrowheads indicate P-MLC in region of TJ. GFP-MLC (A′, green in merge) was mainly localized at basal plasma membrane, nuclei in blue. (B, D, and F) P-MLC in extension (B, 16 h CM), chain (D, 40 h CM), and extension after Y27632 treatement (F, 16 h CM + 30 μM Y27632), respectively. (B) Solid arrows indicate P-MLC associated with basolateral plasma membrane in extension. (D) Open arrowheads indicate P-MLC in cytoplasm of cell in chain. Left open arrow is in leading region of the cell, whereas right open arrow is in trailing region of the cell. (F) Asterisks indicate elongated, narrow extension. (C, E, and G) GFP-MLC in extension (C, 16 h CM), chain (D, 40 h CM), and extension after Y27632 treatment (G, 16 h CM + 30 μM Y27632), respectively. GFP-MLC is primarily located at the basolateral membrane, but some staining is observed apically, near tight junctions (arrowheads). (H) CM and Y27632 do not affect MCL expression levels. Confluent MDCK cells on 24-mm wells remained untreated or were treated for 16 h with CM in absence or presence of 30 μM Y27632, or with Y27632 alone. MLC in whole cell lysates was detected by Western blotting by using an anti-MLC antibody.

In extensions, most of the P-MLC and GFP-MLC are at the elongated basal surface (Figure 4, B and C, solid arrows). In cells in chains, the majority of the P-MLC is in a new location, primarily cytoplasmic (Figure 4D, open arrows). GFP-MLC is primarily still associated with the basolateral membrane. The cytoplasmic P-MLC is both in the "trailing" portion of the cell, i.e., the cytoplasm between the nucleus and the cyst wall and in the "leading" portion of the cell. This relocalization of P-MLC is yet another difference between extensions and chains. When cysts were treated with both CM and Y27632, the P-MLC signal was weaker (Figure 4F), consistent with the idea that Y27632 causes an inhibition of phosphorylation of P-MLC. Some of the P-MLC was in the elongated extensions (Figure 4F, asterisks), which seemed narrower than those formed without Y27632 (e.g., solid arrows in Figure 4B). Due to the apparent narrowness

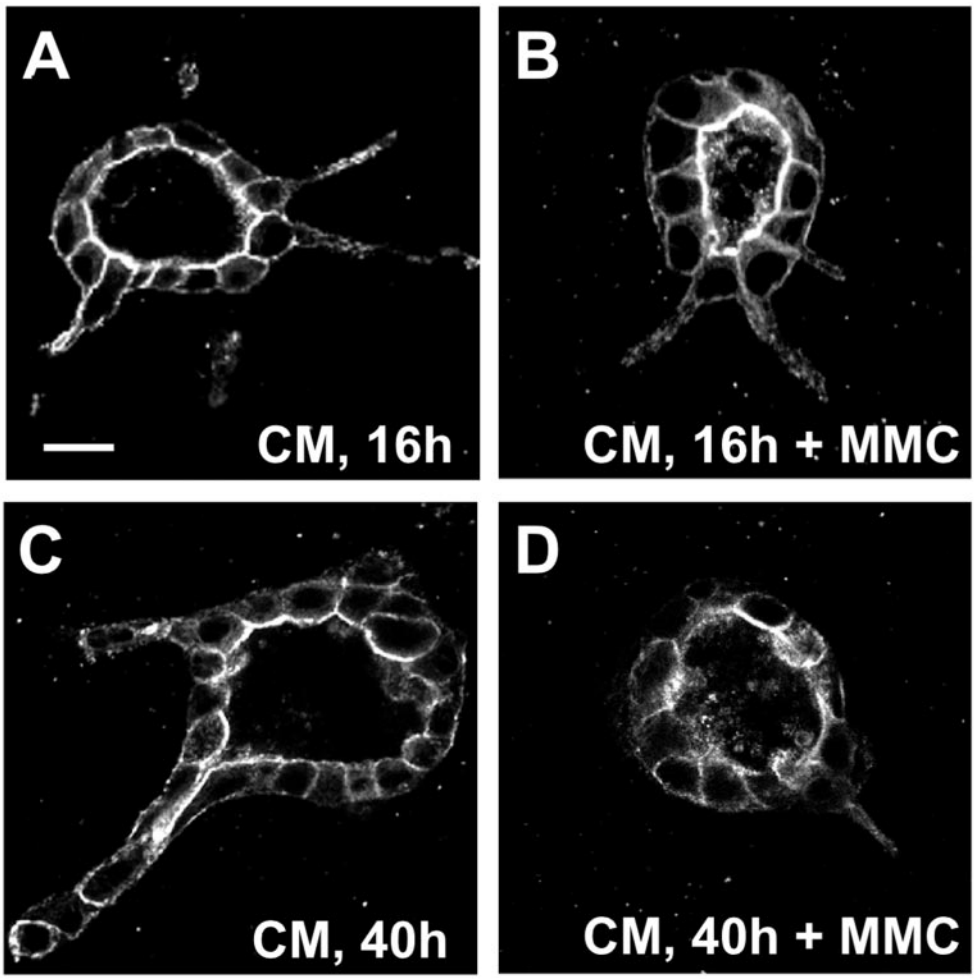

Figure 5. Effect of mitomycin C on extension and chain formation. Cysts were stained with fluorescent phalloidin. (A) Cyst treated with CM for 16 h. (B) Cyst treated with CM and 0.5 μg/ml mitomycin C for 16 h. Note apparently normal extensions. (C) Cyst treated with CM for 40 h to produce chains. (D) Cyst treated with CM and 0.5 μg/ml mitomycin C for 40 h. Note absence of chains.

of the extensions formed in the presence of CM + Y27632, it was difficult to be certain whether the P-MLC was cytoplasmic and/or associated with the inner surface of the plasma membrane of the extension. Some of the P-MLC remained associated with the TJ (Figure 4F, arrowhead). This TJ-associated P-MLC was not appreciably diminished in intensity compared with the TJ-associated P-MLC in control (Figure 4B), suggesting that the TJ-associated P-MLC may be relatively resistant to loss of phosphorylation caused by Y27632.

Taken together, these results suggest that ROCK normally causes contractility of actin-myosin bundles, which acts to inhibit production and elongation of extensions. Blockage of ROCK by Y27632 relieves this inhibition of extensions, resulting in more and longer extensions. Phosphorylation of MLC is likely to be a relevant result of ROCK activity, although other downstream effectors of ROCK may be involved.

Role of Cell Division

The development of some invertebrate tubules, such as the trachea in *Drosophila*, occurs postmitotically (Metzger and Krasnow, 1999; Hogan and Kolodziej, 2002). We investigated whether cell division was necessary for tubulogenesis in the HGF/MDCK system. Apart from enhancing cell motility and cell scattering, HGF is a potent mitogen in a variety of cell types, including filter-grown MDCK cells (Birchmeier and Gherardi, 1998). Indeed, we observed a sixfold increase in mitotic figures in cysts that were treated with CM for 16 h (47 per 100 cysts in CM-treated cells vs. 7 in untreated controls). As shown in Figure 2, nocodazole treatment leads to a block in both cell division and chain formation, which indicates a role for cell division in tubulogenesis. To further analyze the role of cell proliferation in HGF-induced tubulogenesis, we inhibited cell proliferation by preincubating cysts with the cell cycle inhibitor mitomycin C at 37°C overnight. Cysts were then treated with CM in the presence of mitomycin C for an additional 16 h. As was observed with nocodazole, cysts treated with mitomycin C still formed extensions (Figure 5, compare A and B) but tubulogenesis did not proceed, because cysts treated for 40 h with CM in the presence of mitomycin C did not form chains (Figure 5, compare C and D). Moreover, the cysts lost most of their extensions. Importantly, the general polarized structure of the cysts was largely unchanged. This suggests that the treatment with mitomycin C was not completely toxic to the

cells, because toxicity would have resulted in a collapse of cyst structure and cell death, which was also not observed. Similar results were obtained with another inhibitor of the cell cycle, L-mimosine (our unpublished data). These results show that cell division is not required for formation of extensions but is required for the formation of chains.

Location of Cell Division

Where do cells divide during tubulogenesis? In some mammalian systems, such as lung and endothelia, cell division takes place primarily at the tips of the growing tubules and branches (Mollard and Dziadek, 1998; Nogawa *et al.*, 1998; Huang and Ingber, 1999). We analyzed the location of mitotic figures in CM-treated cells. We found that cell division did not occur at specific sites in the tubule. A typical result is shown in Figure 6, which displays three confocal sections (taken at intervals of 4 μm) of the same branching tubule, which contained several mitotic cells. Of these mitotic cells, one was at the tip of tubule (cell a), two at the base (cells d and e, both of which are late in mitosis), and several were located in the middle of the tubule (cells b, c, and f). This result demonstrates that the tubules can grow by cell proliferation along the whole tubule.

Orientation of Cell Division during Chain Formation

The orientation of cell division plays an important role in morphogenesis in several systems. This has mainly been studied in genetically tractable, such as yeast, *Caenorhabditis elegans*, and *Drosophila* (Jan and Jan, 2001; Knoblich, 2001; Wodarz, 2002). Oriented division also plays a role in neurogenesis in the mammalian brain and during wound healing (Chenn and McConnell, 1995; Heins *et al.*, 2001; Estivill-Torrus *et al.*, 2002; Song *et al.*, 2002). We investigated whether the orientation of cell division could play a role during tubulogenesis. We concentrated on the initial step in formation of chains, in which a cell first leaves the monolayer of the cyst wall.

The orientation of the spindle and the axis of division during mitosis of MDCK cells grown on filters has been reported previously (Reinsch and Karsenti, 1994). To summarize, the centriole in interphase MDCK cells is located just beneath the center of the apical surface. This centriole duplicates and in early prophase, one of the centrioles moves to the basal side of the nucleus. By early prophase, the early spindle forms, with its axis parallel to the apical-basal axis of the cell, i.e., perpendicular to the plane of the monolayer. In prometaphase, the spindle starts a rotation of 90°, so that by metaphase the spindle is now parallel to the plane of the monolayer. The spindle remains in this position until mitosis is completed, so that both daughter cells remain in the plane of the monolayer.

We first analyzed spindle orientation in dividing cells in cysts that were not treated with HGF. (To follow this in live cells, we established a stable MDCK cell line expressing GFP-α-tubulin and collected time-lapse images by confocal microscopy.)

In all cells we analyzed, the spindle rotates by 90° from parallel to the apical-basal axis (Figure 7A, 0′) to parallel to the plane of the monolayer (Figure 7A, 15′), much like cells on a filter. The spindle remains parallel to the monolayer until division is complete.

In contrast, HGF-treated cysts displayed a wide range of degree and type of rotation. Some cells behaved much like untreated cysts, i.e., they underwent a 90° rotation in spindle axis, so that both daughter cells remained in the plane of the monolayer. (Figure 7B).

However, in some HGF-treated dividing cells the spindle did not undergo a 90° rotation and one of the daughter cells apparently left the plane of the monolayer. For instance, in Figure 7C, the spindle failed to rotate from its apical-basal orientation but did undergo small excursions. In other cases (Figure 7D), the spindle underwent larger excursions, e.g., seesaw movement, oscillating back and forth around the apical-basal axis. At 0 min the spindle was parallel to the apical-basal axis, as indicated by the solid line in Figure 7D. The spindle first rotated away from the apical-basal axis in a counterclockwise direction, with a maximum excursion of ~70° at 7 min. However, the spindle then rotated in the opposite direction, reaching ~45° rotation in the opposite direction at 25 min. The spindle then apparently rotated partially out the plane of the section. It should be kept in mind that the spindle may be rotating in three dimensions, and so only part of its rotation may be evident in the our time-lapse images, which are all in one plane of focus. Pronounced three-dimensional rotation has been seen also in the developing mammalian brain (Adams, 1996).

Taken together, these data are consistent with the hypothesis that in the absence of HGF, a spindle rotation mechanism normally ensures that both daughters remain in the monolayer. In contrast, HGF treatment causes an apparently variable loss of this mechanism.

We also examined the effect of Y27632 on spindle orientation in cysts without HGF. We found that the effects to be variable. In Figure 8A, a spindle is observed at 0 min oriented parallel to the monolayer, and this rotates to perpendicular to the monolayer by 25 min. This cell seems to be delayed in mitosis, which is not completed by 86 min. Figure 8B shows a very different pattern, where the spindle seesaws approximately perpendicular to the monolayer (16 and 36 min) and eventually divides, with the cell possibly leaving the monolayer (60 min). It is possible that these variable defects in spindle orientation could account for the effects we saw of Y27362 alone on cyst morphology, such as the spikes seen at 24 h. However, these spikes largely do not seem to involve cells that have divided, but rather seem more likely due to changes in the actin cytoskeleton. These spindle orientation defects may also account, at least in part, for some the effects seen with combined treatment with Y27632 and HGF, such as the isolated cells seen at long time points, and perhaps even the increased number of extensions (though these were more likely produced without mitosis).

DISCUSSION

Our basic result is that MDCK cells in collagen exhibit two types of polarization and movement, and that HGF induces the cells to switch from one type to the other as the cells make the transition from extensions to chains. Cells with extensions resemble the apparently nonmotile polarized ep-

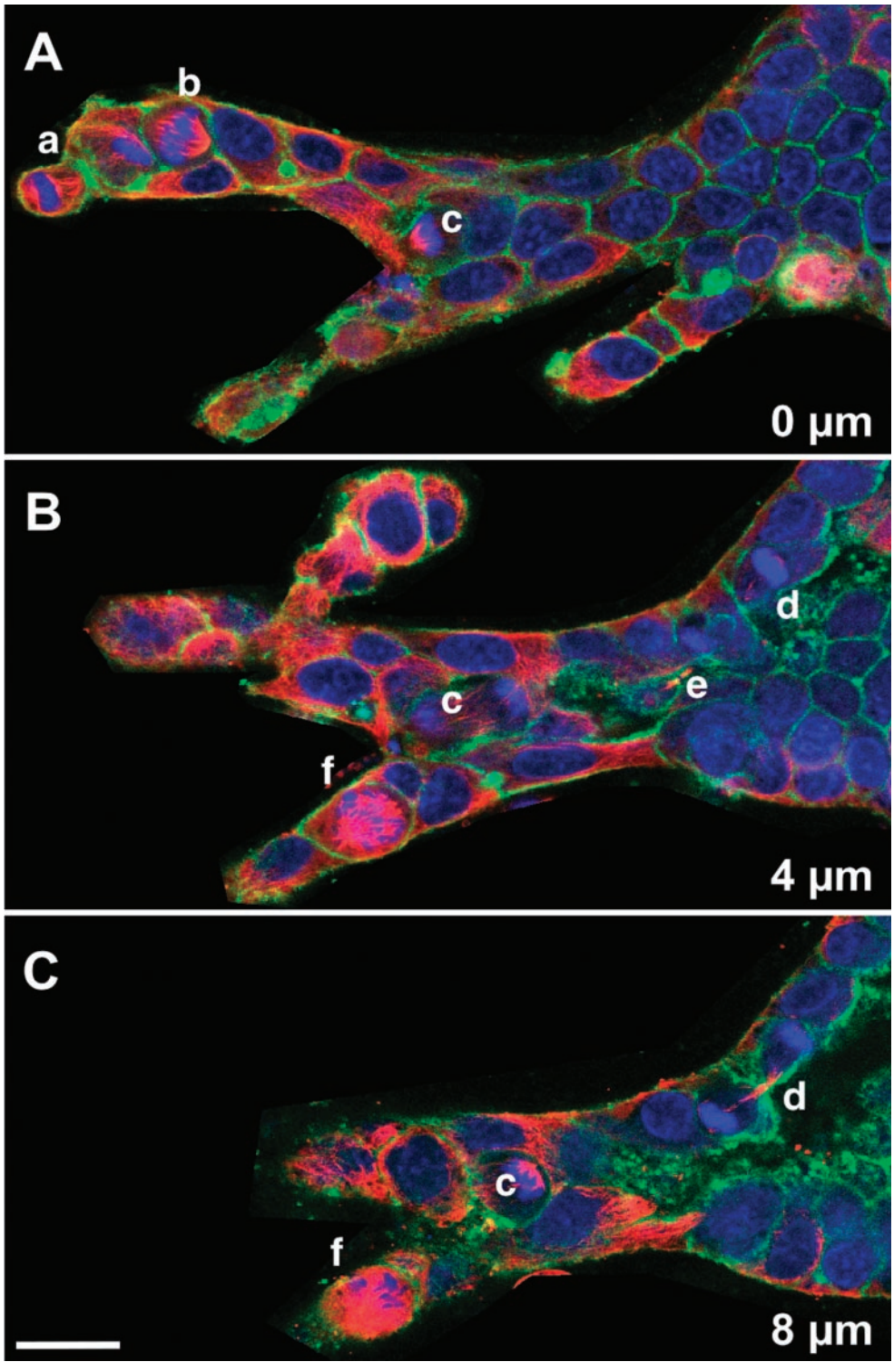

Figure 6. Location of cell division. (A, B, and C) Three serial confocal sections, 4 μm apart, of a complex branching structure in a cyst stimulated with CM for 72 h, followed by 24 h with CM and 200 ng/ml nocodazole (to accumulate cells in mitosis). Red is immunofluorescence staining for α-tubulin, green is fluorescent phalloidin, and blue is nuclei. Individual mitotic cells are indicated by lowercase letters; some of these cells are visible in more than one section.

ithelial cells in the monolayer in that they still have apical-basolateral polarity. However, these cells have a type of movement, i.e., they protrude a pseudopodial extension. In contrast, MDCK cells in chains have lost almost all remnants of epithelial polarity and instead resemble other typical migrating cells, such as migrating fibroblasts.

PI3K is required for both the initiation and maintenance of extensions. As was observed in the leading edges of fibro-

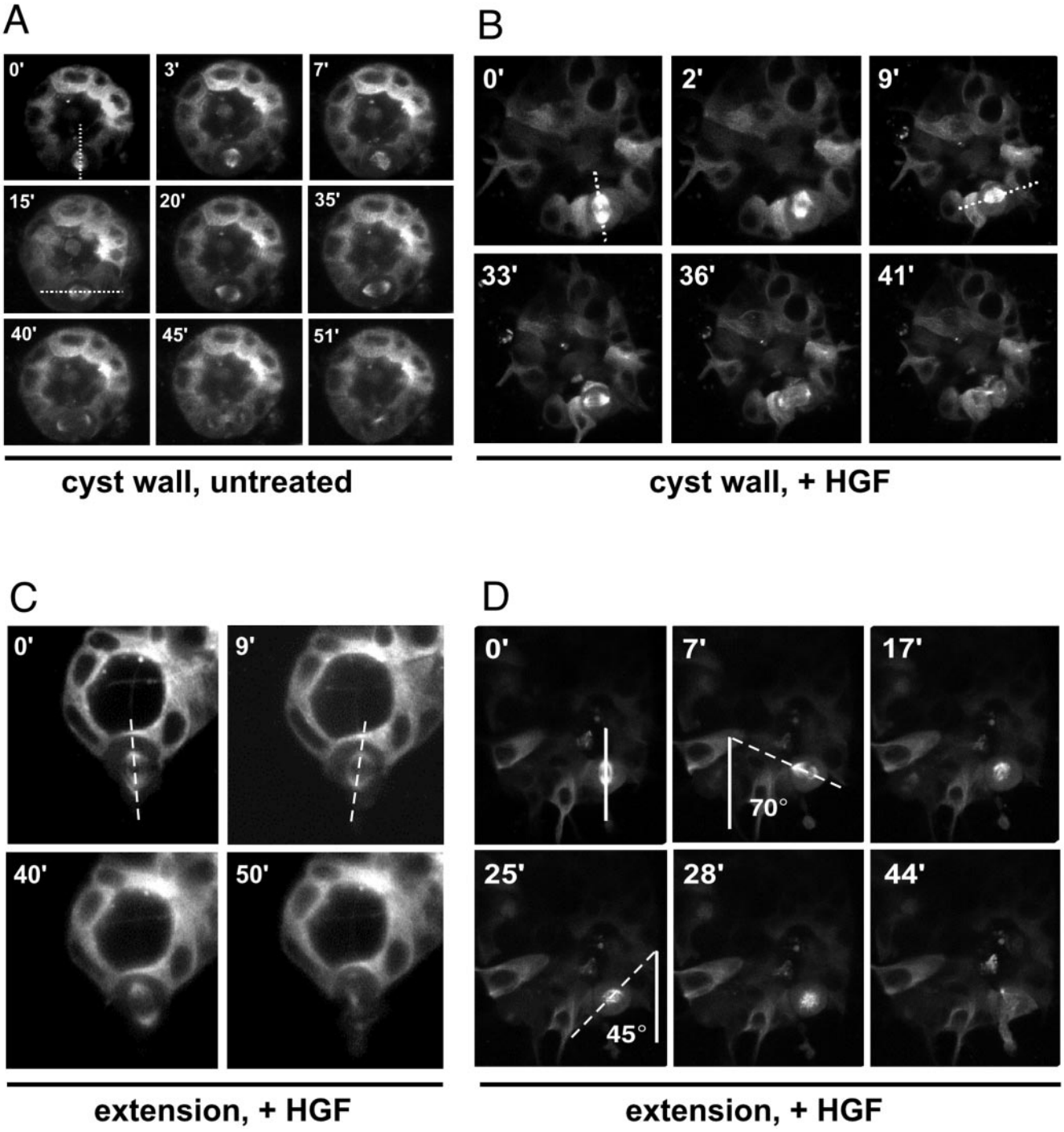

Figure 7. Time-lapse images of orientation of mitotic spindle. All images are of cysts expressing GFP-α-tubulin, taken by time-lapse confocal microscopy. (A) Untreated cyst. The mitotic spindle is oriented in the apical-basal axis at 0 min (dotted line), rotates 90° to the plane of the monolayer by 15 min, and remains in this orientation through the completion of mitosis. (B) Cyst treated with CM. The mitotic spindle is oriented in the apical-basal axis at 0 min (dotted line) and rotates to the plane of the monolayer by 9 min. In this case, the spindle axis remains in this orientation through the completion of mitosis and the cell does not leave the monolayer. (C) Cyst treated with CM. This spindle exhibits little rotation and remains parallel to the apical-basal axis. (D) Cyst treated with CM. This cyst exhibits seesawing motion of spindle. The spindle is oriented in the apical-basal axis at 0 min (solid line). It first rotates counterclockwise to 70° at 7 min (dotted line). The spindle then rotates clockwise, passing through the apical-basal axis at 17 min and reaches 45° in the opposite direction at 25 min. Eventually, the spindle rotates out of the plane of focus.

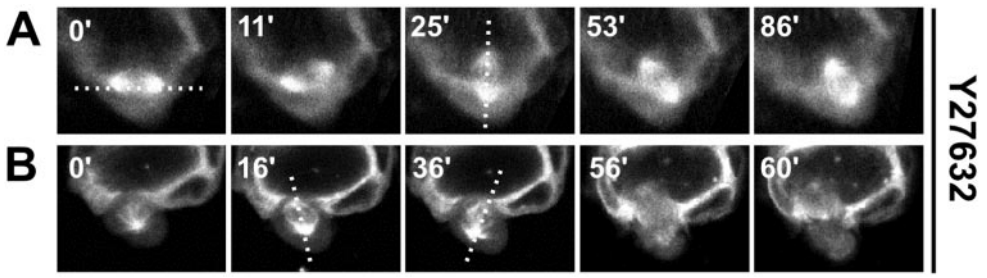

Figure 8. Effect of inhibition of ROCK on spindle orientation of cyst. Images are of live cysts expressing GFP-α-tubulin, taken by time lapse confocal microscopy. (A) In cysts treated with 30 μM Y27632 for 24 h, the spindle axis rotates 90°, from perpendicular to apical-basal axis (at 0′) to parallel to apical-basal axis at 25′). Cell division was not completed after 86′. (B) This spindle exhibits little rotation in the apical-basal axis and finally divides in the apical-basal axis.

blasts, neutrophils, and *Dictyostelium*, lipid products of PI3K accumulate in HGF-induced extensions. Moreover, inhibition of PI3K activity with LY294002 blocks extension formation. Presumably, PI3K plays a similar role to that in neutrophils and *Dictyostelium*, where it provides an intracellular signal for the direction of migration. However, not all cell migration depends on PI3K, e.g., the long pseudopodial extensions that astrocytes form in direction of migration during wound healing resemble MDCK extensions (both are long, large, and relatively slowly moving) but are not affected by PI3K inhibitors (Etienne-Manneville and Hall, 2001).

Cells that change direction quickly, e.g., neutrophils, do not rely on the relatively slow polarization of the Golgi or MTs (Schliwa and Hõner, 1993) but rather depend on rearrangements of the actin cytoskeleton. In contrast, cells that form pseudopodia slowly and move slowly, e.g., astrocytes, rely more on MTs for movement, and astrocyte polarization and pseudopod formation do not depend on actin polymerization (Etienne-Manneville and Hall, 2001). MDCK extension formation is, like pseudopod formation in astrocytes, much slower than neutrophil migration (time scale of hours rather than minutes). It is therefore surprising that extension formation does not rely on MT dynamics or Golgi reorientation but does depend on actin polymerization.

From this viewpoint, extensions somewhat resemble neutrophils, because they require PI3K and actin, but do not involve Golgi reorientation or MT. In contrast, chain formation involves Golgi reorientation, and thus resembles fibroblasts and astrocytes. It was difficult to assess the role of PI3K and polymerized actin in chains, because their inhibitors led to a collapse of extensions, which are the precursors of chains. It was also hard to assess the role of MT dynamics in chains, because the nocodazole inhibits mitosis, which is necessary for chain formation.

The differences between formation of extensions and chains have in vivo parallels. In the development of salivary glands and trachea in *Drosophila*, cells first send out pseudopodial extensions, and then the entire epithelial cell moves. Mutation of the *ribbon* gene does not prevent extension formation by these developing gland cells but does prevent movement of the cell bodies, which may be analogous to chain formation in the MDCK system (Bradley and Andrew, 2001; Shim *et al.*, 2001).

ROCK Controls the Number and Length of Extensions

It is not known what controls the number or length of extensions or tubules. Even though cysts are uniformly exposed to HGF and all of the cells are theoretically capable of responding, only a minority of cells in the cyst produce extensions and then tubules. Y27632 greatly increased the number and length of HGF-induced extensions and produced very small extensions on its own. These effects are compatible to previous data that activation of Rho inhibits HGF-induced scattering of MDCK cells (Ridley *et al.*, 1995). Inhibition of ROCK also produces extensions (neurites) in neuroblastoma cells and pseudopodia in fibroblasts (Hirose *et al.*, 1998) and increases the rate of fibroblast movement in a wound-healing assay (Nobes and Hall, 1999). Our data suggest that normally ROCK (and presumably the contractility and stress fibers that it controls) inhibits movement and pseudopod formation in a number of systems, including MDCK cell extensions.

ROCK activity leads to the production of P-MLC, which in turn promotes actin-myosin contractility. We find that in cells in the monolayer of the cyst wall, most of the P-MLC underlies the basal surface, with some in the region of the tight junction. During extension formation the P-MLC remains underneath the elongated basal surface. However, a completely different localization of P-MLC is seen in chains, where most of the P-MLC is diffuse in the cytoplasm, especially the trailing region of the cytoplasm. This trailing location is similar to that seen in migrating neutrophils, where P-MLC is predominantly located in the tail or uropod of the migrating neutrophil (J. Xu, F. W. and H. B., unpublished). Indeed, ROCK is needed for detachment of the uropod in migrating leukocytes (Alblas *et al.*, 2001; Worthylake *et al.*, 2001).

Ordinarily, in response to HGF, cells move centripetally away from the cysts, whereas with Y27632, some cells move toward the center. This may be due to disruption of the mechanism that normally causes cells to move in only one direction, toward the source of HGF. Intriguingly, a similar effect is seen with Y27632 treatment of neutrophils, which produces multiple pseudopods in random directions (Wang and Bourne, unpublished data). We cannot exclude other possibilities, e.g., that Y27632 makes tight junctions leaky, allowing cells to chemotax toward HGF that has leaked into the lumen (Walsh *et al.*, 2001).

Role of Cell Division in Tubulogenesis

Most tubulogenesis in vertebrates involves cell proliferation (Hogan and Kolodziej, 2002). Consistent with that, we found that inhibition of MDCK cell division blocked chain formation, though extensions were not affected.

Orientated cell divisions play a crucial role in many steps in development. Cells in the wall of unstimulated cysts behave similarly to those grown on a filter support. The spindle forms parallel to the apical-basal axis and then consistently rotates 90° to be parallel to the plane of the monolayer. In striking contrast, with HGF treatment the rotation was highly variable. Some spindles underwent almost no rotation, some rotated normally, and some had large seesaw excursions. A similar type of seesaw motion has been observed in oriented cell division in *Drosophila melanogaster* (Lu *et al.*, 2001; Roegiers *et al.*, 2001). Our results suggest that the mechanism that normally rotates the spindle and produces coplanar division is variably lost with HGF treatment. This causes some daughter cells to leave the monolayer and perhaps initiate or contribute to a chain.

Superficially, at least, the reorientation of cell division in MDCK cells resembles the orientation of cell division in *Drosophila* neurogenesis. Neuroblasts arise from an epithelium, where some cells divide in the plane of the monolayer and thereby remain in this monolayer. Recent evidence indicates that the orientation of the spindle is controlled by a hierarchical mechanism (Lu *et al.*, 2001; Roegiers *et al.*, 2001). The default situation in the *Drosophila* system is for the spindle to orient in the apical-basal direction. A superimposed signal involving the adherens junction can orient the spindle parallel to the plane of the monolayer. When viewed in this context, our data suggest a model wherein normal division of MDCK in a monolayer, the spindle rotates 90° because it is captured into a position parallel to the monolayer. This capture mechanism may involve the interaction of astral microtubules with a protein associated with the adherens junctions. We suggest that during HGF-induced tubulogenesis, this normal capture mechanism may be abrogated in some (but not all) cells. The result could be that the spindle is not anchored in any particular orientation and in some cases can undergo a seesaw motion.

MDCK tubulogenesis may provide an accessible system to dissect the mechanisms of orientation of cell division in mammalian cells. Proteins that have been suggested to play roles in controlling orientation of the spindle and cell division in mammalian cells and are therefore possible targets for HGF-induced reorientation of division include LIS1 (Faulkner *et al.*, 2000), PINS (partner of inscuteable), NuMA (Du *et al.*, 2001), dynein, EB1, and APC (adenomatous polyposis coli) (Dujardin and Vallee, 2002; Gundersen, 2002). We also found that inhibition of ROCK leads to variable defects in spindle orientation and rotation, suggesting that ROCK may be involved in this process. Our results raise the possibility that orientation of cell division may play a role in tubulogenesis, and therefore is potentially important both during development and during tubulogenesis in adults, which occurs during normal physiology (e.g., cycling of mammary andendometrial glands), regeneration (e.g., after renal tubular necrosis), and pathological proliferation of tubules (e.g., hypersecretory lung diseases).

ACKNOWLEDGMENTS

We thank Bill Hyun and the University of California, San Francisco, Mt. Zion Cancer Center, for access to a Zeiss 510 confocal microscope. One of the Zeiss 510 confocal microscopes was supported by the University of California, San Francisco-Sandler Family Fund for New Technologies and California Cancer Research Agency. We thank Drs. Ralph Schwall (Genentech), for a gift of rhHGF and Kathleen Kennedy (National Cancer Institute) for permission to use the GFP-MLC construct. We thank Dr. Anirban Datta (University of California, San Francisco) for permission to cite unpublished results. We thank Jeanette Wong for assistance with manuscript preparation. W.Y. was supported by fellowship from the California American Heart Association (0120084Y). M.Z. was supported by a fellowship of the California Division of the American Cancer Society (2-7-99). F.W. is supported by National Institutes of Health training grant HL07713. Work in H.B.'s laboratory is supported by National Institutes of Health GM-27800. Work in K.M.'s laboratory is supported by National Institutes of Health grants and by the Sandler Center for Basic Research in Asthma.

REFERENCES

Adams, R.J. (1996). Metaphase spindles rotate in the neuroepithelium of rat cerebral cortex. J. Neurosci. *16*, 7610–7618.

Alblas, J., Ulfman, L., Hordijk, P., and Koenderman, L. (2001). Activation of Rhoa and ROCK are essential for detachment of migrating leukocytes. Mol. Biol. Cell *12*, 2137–2145.

Amano, M., Ito, M., Kimura, K., Fukata, Y., Chihara, K., Nakano, T., Matsuura, Y., and Kaibuchi, K. (1996). Phosphorylation and activation of myosin by Rho-associated kinase (Rho-kinase). J. Biol. Chem. *271*, 20246–20249.

Arias, A.M. (2001). Epithelial mesenchymal interactions in cancer and development. Cell *105*, 425–431.

Birchmeier, C., and Gherardi, E. (1998). Developmental roles of HGF/SF and its receptor, the c-Met tyrosine kinase. Trends Cell Biol. *8*, 404–410.

Bishop, A.L., and Hall, A. (2000). Rho GTPases, and their effector proteins. Biochem. J. *348 Pt 2*, 241–255.

Bradley, P.L., and Andrew, D.J. (2001). *ribbon* encodes a novel BTB/POZ protein required for directed cell migration in *Drosophila melanogaster*. Development *128*, 3001–3015.

Breitfeld, P., Casanova, J.E., Harris, J.M., Simister, N.E., and Mostov, K.E. (1989). Expression and analysis of the polymeric immunoglobulin receptor. Methods Cell Biol. *32*, 329–337.

Chenn, A., and McConnell, S.K. (1995). Cleavage orientation and the asymmetric inheritance of Notch1 immunoreactivity in mammalian neurogenesis. Cell *82*, 631–641.

Chrzanowska-Wodnicka, M., and Burridge, K. (1996). Rho-stimulated contractility drives the formation of stress fibers and focal adhesions. J. Cell Biol. *133*, 1403–1415.

Comer, F.I., and Parent, C.A. (2002). PI 3-Kinases and PTEN. How opposites chemoattract. Cell *109*, 541–544.

Comoglio, P.M., and Boccaccio, C. (2001). Scatter factors and invasive growth. Semin. Cancer Biol. *11*, 153–165.

Cukierman, E., Pankov, R., Stevens, D.R., and Yamada, K.M. (2001). Taking cell-matrix adhesions to the third dimension. Science *294*, 1708–1712.

Drubin, D.G., and Nelson, W.J. (1996). Origins of cell polarity. Cell *84*, 335–344.

Du, Q., Stukenberg, P.T., and Macara, I.G. (2001). A mammalian partner of inscuteable binds NuMA and regulates mitotic spindle organization. Nat. Cell Biol. *3*, 1069–1075.

Dujardin, D.L., and Vallee, R.B. (2002). Dynein at the cortex. Curr. Opin. Cell Biol. *14*, 44–49.

Estivill-Torrus, G., Pearson, H., van Heyningen, V., Price, D.J., and Rashbass, P. (2002). Pax6 is required to regulate the cell cycle and the rate of progression from symmetrical to asymmetrical division in mammalian cortical progenitors. Development *129*, 455–466.

Etienne-Manneville, S., and Hall, A. (2001). Integrin-mediated activation of Cdc42 controls cell polarity in migrating astrocytes through PKCξ. Cell *106*, 489–498.

Faulkner, N.E., Dujardin, D.L., Tai, C.Y., Vaughan, K.T., O'Connell, C.B., Wang, Y., and Vallee, R.B. (2000). A role for the lissencephaly gene LIS1 in mitosis and cytoplasmic dynein function. Nat. Cell Biol. *2*, 784–791.

Firtel, R.A., and Chung, C.Y. (2000). The molecular genetics of chemotaxis: sensing and responding to chemoattractant gradients. Bioessays *22*, 603–615.

Franz, C.M., Jones, G.E., and Ridley, A.J. (2002). Cell migration in development and disease. Dev. Cell *2*, 153–158.

Gundersen, G.G. (2002). Evolutionary conservation of microtubule-capture mechanisms. Nat. Rev. Mol. Cell. Biol. *3*, 6–14.

Haugh, J.M., Codazzi, F., Teruel, M., and Meyer, T. (2000). Spatial sensing in fibroblasts mediated by 3′ phosphoinositides. J. Cell Biol. *151*, 1269–1280.

Heins, N., Cremisi, F., Malatesta, P., Gangemi, R.M., Corte, G., Price, J., Goudreau, G., Gruss, P., and Gotz, M. (2001). Emx2 promotes symmetric cell divisions and a multipotential fate in precursors from the cerebral cortex. Mol. Cell. Neurosci. *18*, 485–502.

Hirose, M., Ishizaki, T., Watanabe, N., Uehata, M., Kranenburg, O., Moolenaar, W.H., Matsumura, F., Maekawa, M., Bito, H., and Narumiya, S. (1998). Molecular dissection of the Rho-associated protein kinase (p160ROCK)-regulated neurite remodeling in neuroblastoma N1E-115 cells. J. Cell Biol. *141*, 1625–1636.

Hogan, B.L.M., and Kolodziej, P.A. (2002). Organogenesis: molecular mechanisms of tubulogenesis. Nat. Rev. Genet. *3*, 513–523.

Huang, S., and Ingber, D.E. (1999). The structural and mechanical complexity of cell-growth control. Nat. Cell Biol. *1*, E131–E138.

Jan, Y.N., and Jan, L.Y. (2001). Asymmetric cell division in the *Drosophila* nervous system. Nat. Rev. Neurosci. *2*, 772–779.

Kamikura, D.M., Khoury, H., Maroun, C., Naujokas, M.A., and Park, M. (2000). Enhanced transformation by a plasma membrane-associated met oncoprotein: activation of a phosphoinositide 3′-kinase-dependent autocrine loop involving hyaluronic acid and CD44. Mol. Cell. Biol. *10*, 3482–3496.

Khwaja, A., Lehmann, K., Marte, B.M., and Downward, J. (1998). Phosphoinositide 3-kinase induces scattering and tubulogenesis in epithelial cells through a novel pathway. J. Biol. Chem. *273*, 18793–18801.

Kimura, K., *et al*. (1996). Regulation of myosin phosphatase by Rho and Rho-associated kinase (Rho-kinase). Science *273*, 245–248.

Knoblich, J.A. (2001). Asymmetric cell division during animal development. Nat. Rev. Mol. Cell. Biol. *2*, 11–20.

Lipschutz, J.H., Guo, W., O'Brien, L.E., Nguyen, Y.H., Novick, P., and Mostov, K.E. (2000). Exocyst is involved in cystogenesis and tubulogenesis and acts by modulating synthesis and delivery of basolateral plasma membrane and secretory proteins. Mol. Biol. Cell *11*, 4259–4275.

Lipschutz, J.H., O'Brien, L.E., Altschuler, Y., Avrahami, D., Nguyen, Y., Tang, K., and Mostov, K.E. (2001). Analysis of membrane traffic in polarized epithelial cells. Curr. Prot. Cell Biol. *15*, 5.

Lu, B., Roegiers, F., Jan, L.Y., and Jan, Y.N. (2001). Adherens junctions inhibit asymmetric division in the *Drosophila* epithelium. Nature *409*, 522–525.

Metzger, R.J., and Krasnow, M.A. (1999). Genetic control of branching morphogenesis. Science *284*, 1635–1639.

Mollard, R., and Dziadek, M. (1998). A correlation between epithelial proliferation rates, basement membrane component localization patterns, and morphogenetic potential in the embryonic mouse lung. Am. J. Respir. Cell Mol. Biol. *19*, 71–82.

Montesano, R., Matsumoto, K., Nakamura, T., and Orci, L. (1991a). Identification of a fibroblast-derived epithelial morphogen as hepatocyte growth factor. Cell *67*, 901–908.

Montesano, R., Schaller, G., and Orci, L. (1991b). Induction of epithelial tubular morphogenesis in vitro by fibroblast-derived soluble factors. Cell *66*, 697–711.

Mostov, K.E., Verges, M., and Altschuler, Y. (2000). Membrane traffic in polarized epithelial cells. Curr. Op. Cell Biol. *12*, 483–490.

Nabi, I.R. (1999). The polarization of the motile cell. J. Cell Sci. *112*, 1803–1811.

Nobes, C.D., and Hall, A. (1999). Rho GTPases control polarity, protrusion, and adhesion during cell movement. J. Cell Biol. *144*, 1235–1244.

Nogawa, H., Morita, K., and Cardoso, W.V. (1998). Bud formation precedes the appearance of differential cell proliferation during branching morphogenesis of mouse lung epithelium in vitro. Dev. Dyn. *213*, 228–235.

O'Brien, L.E., Jou, T.S., Pollack, A.L., Zhang, Q., Hansen, S.H., Yurchenco, P., and Mostov, K.E. (2001). Rac1 orientates epithelial apical polarity through effects on basolateral laminin assembly. Nat. Cell Biol. *3*, 831–838.

O'Brien, L.E., Zegers, M.M.P., and Mostov, K.E. (2002). Opinion. Building epithelial architecture: insights from three-dimensional culture models. Nat. Rev. Mol. Cell. Biol. *3*, 531–537.

Pollack, A.L., Barth, A.I., Altschuler, Y., Nelson, W.J., and Mostov, K.E. (1997). Dynamics of beta-catenin interactions with APC protein regulate epithelial tubulogenesis. J. Cell Biol. *137*, 1651–1662.

Pollack, A.L., Runyan, R.B., and Mostov, K.E. (1998). Morphogenetic mechanisms of epithelial tubulogenesis: MDCK cell polarity is transiently rearranged without loss of cell-cell contact during scatter factor/hepatocyte growth factor-induced tubulogenesis. Dev. Biol. *204*, 64–79.

Reinsch, S., and Karsenti, E. (1994). Orientation of spindle axis and distribution of plasma membrane proteins during cell division in polarized MDCKII cells. J. Cell Biol. *126*, 1509–1526.

Ridley, A.J. (2001). Rho family proteins: coordinating cell responses. Trends Cell Biol. *11*, 471–477.

Ridley, A.J., Comoglio, P.M., and Hall, A. (1995). Regulation of scatter factor/hepatocyte growth factor responses by Ras, Rac, and Rho in MDCK cells. Mol. Cell. Biol. *15*, 1110–1122.

Roegiers, F., Younger-Shepherd, S., Jan, L.Y., and Jan, Y.N. (2001). Two types of asymmetric divisions in the Drosophila sensory organ precursor cell lineage. Nat. Cell Biol. *3*, 58–67.

Savagner, P. (2001). Leaving the neighborhood: molecular mechanisms involved during epithelial-mesenchymal transition. Bioessays *23*, 912–923.

Schliwa, M., and Hõner, B. (1993). Microtubules, centrosomes and intermediate filaments in directed cell movement. Trends Cell Biol. *3*, 377–380.

Servant, G., Weiner, O.D., Herzmark, P., Balla, T., Sedat, J.W., and Bourne, H.R. (2000). Polarization of chemoattractant receptor signaling during neutrophil chemotaxis. Science *287*, 1037–1040.

Shim, K., Blake, K.J., Jack, J., and Krasnow, M.A. (2001). The *Drosophila* ribbon gene encodes a nuclear BTB domain protein that promotes epithelial migration and morphogenesis. Development *128*, 4923–4933.

Song, B., Zhao, M., Forrester, J.V., and McCaig, C.D. (2002). Electrical cues regulate the orientation and frequency of cell division and the rate of wound healing in vivo. Proc. Natl. Acad. Sci. USA *99*, 13577–13582.

Stowers, L., Yelon, D., Berg, L.J., and Chant, J. (1995). Regulation of the polarization of T cells toward antigen-presenting cells by Ras-related GTPase CDC42. Proc. Natl. Acad. Sci. USA *92*, 5027–5031.

Uehata, M., *et al*. (1997). Calcium sensitization of smooth muscle mediated by a Rho-associated protein kinase in hypertension. Nature *389*, 990–994.

Vasquez, R.J., Howell, B., Yvon, A.M., Wadsworth, P., and Cassimeris, L. (1997). Nanomolar concentrations of nocodazole alter microtubule dynamic instability in vivo and in vitro. Mol. Biol. Cell *8*, 973–985.

Walsh, S.V., Hopkins, A.M., Chen, J., Narumiya, S., Parkos, C.A., and Nusrat, A. (2001). Rho kinase regulates tight junction function and is necessary for tight junction assembly in polarized intestinal epithelia. Gastroenterology *121*, 566–579.

Wang, F., Herzmark, P., Weiner, O.D., Srinivasan, S., Servant, G., and Bourne, H.R. (2002). Lipid products of PI(3)Ks maintain persistent cell polarity and directed motility in neutrophils. Nat. Cell Biol. *4*, 513–518.

Ward, Y., Yap, S.F., Ravichandran, V., Matsumura, F., Ito, M., Spinelli, B., and Kelly, K. (2002). The GTP binding proteins Gem and Rad are negative regulators of the Rho-Rho kinase pathway. J. Cell Biol. *157*, 291–302.

Watton, S.J., and Downward, J. (1999). Akt/PKB localization and 3′ phosphoinositide generation at sites of epithelial cell-matrix and cell-cell interaction. Curr. Biol. *9*, 433–436.

Webb, D.J., Parsons, J.T., and Horwitz, A.F. (2002). Adhesion assembly, disassembly and turnover in migrating cells - over and over and over again. Nat. Cell Biol. *4*, E97–E100.

Wittmann, T., and Waterman-Storer, C.M. (2001). Cell motility: can Rho GTPases and microtubules point the way? J. Cell Sci. *114*, 3795–3803.

Wodarz, A. (2002). Establishing cell polarity in development. Nat. Cell Biol. *4*, E39–E44.

Worthylake, R.A., Lemoine, S., Watson, J.M., and Burridge, K. (2001). RhoA is required for monocyte tail retraction during transendothelial migration. J. Cell Biol. *154*, 147–160.

Yvon, A.M., Walker, J.W., Danowski, B., Fagerstrom, C., Khodjakov, A., and Wadsworth, P. (2002). Centrosome reorientation in wound-edge cells is cell type specific. Mol. Biol. Cell *13*, 1871–1880.

Zegers, M.M.P., O'Brien, L.E., Yu, W., Datta, A., and Mostov, K.E. (2003). Epithelial polarity and tubulogenesis in vitro. Trends Cell Biol. (*in press*).